Defence Science Journal, Vol. 67, No. 5, September 2017, pp. 487-496, DOI : 10.14429/dsj.67.11087

Investigation of Incompressible Flow Past Two Circular Cylinders of Different Diameters

Y.G. Bhumkar[!], P. Kumar[#,*], A. Roy[@], S. Das[#], and J.K. Prasad[#]

[!]*Department of Mechanical Engineering, Indian Institute of Technology Bhubaneshwar - 751 013, India*
[@]*Department of Aerospace Engineering, Indian Institute of Technology Kharagpur- 721 302, India*
[#]*Department of Space Engineering and Rocketry, Birla Institute of Technology, Mesra, Ranchi -835 215, India*
[*]*E-mail: priyankkumar@bitmesra.ac.in*

ABSTRACT

A two - dimensional Navier-Stokes solver based on finite volume approach using a boundary-fitted curvilinear structured O-grid has been developed to obtain details of unconfined flow past cylinders at low Reynolds number of 100 and 200 based on diameter. Computations made on a single cylinder with smaller domain adopting the convective boundary conditions captured most of the flow features. This concept of a smaller domain, when used to capture the highly complex flow field around two cylinders of the same diameter placed in tandem at a Reynolds number of 200 showed reasonable results. The details of the flow field around two cylinders of different diameters placed at a typical distance of 3L and Reynolds number of 100 could be well captured adopting smaller domain concept. It is observed that the change in diameter of upstream cylinder strongly influences the overall flow field and the drag of the downstream cylinder.

Keywords: Two-dimensional cylinders; Two cylinders in tandem; Different diameter cylinders; Incompressible flow

NOMENCLATURE

A	Area of the control volume
C_{D1}, C_{D2}	Drag coefficient of upstream and downstream cylinder
C_{L1}, C_{L2}	Lift coefficient of upstream and downstream cylinder
G	Distance between centers of two cylinders
M, N	Number of grid cells along ξ- andη-directions
$E, NE, N, NW, W, SW, S, SE, EE, NN, WW, SS$	Cells surrounding the control volume P
$r_{1,2}, r_{2,3}, ...$	Line segment from point 1 to 2, etc.
p	Pressure
Re	Reynolds number
D_1, D_2	Diameter of upstream and downstream cylinder
L	Average of diameter of two cylinders [$(D_1 + D_2)/2$]
St	Strouhal number
u,v	Velocities
U_∞	Freestream velocity
V_ξ , V_η	Grid aligned velocity components
v_r, v_θ	Radial and circumferential velocities
av	Time averaged
1, 2, 3, 4	Nodes of main control volume P
e, n, s, w	Cell face centres of the east, north, west and south faces of main control volume P
n	Time step
ξ, η	Grid aligned directions
θ_C	Angular orientation of a point on circular cylinder surface
Ω	Two-dimensional flow domain
ϕ	Transport property
ε	Turbulent dissipation
Δ	Spacing operator, e.g. $\Delta x_{12} = x_2 - x_1$
Δt, δt	Time step
ω_w	Wall vorticity
Γ	Circulation

Received : 02 March 2017, Revised : 29 June 2017
Accepted : 27 July 2017, Online published : 19 September 2017

1. INTRODUCTION

Flow past two-dimensional circular cylinder has been extensively studied due to its practical importance and variety of applications in real life such as heat exchanger, high rise chimneys, and buildings, offshore structures, cooling towers of nuclear establishments, transmission cables, etc. The flow around a circular cylinder involves flow separation, massively separated wakes which increase the complexity of the flow. These flow are highly unsteady and complicated due to which the determination of the separation location of the flow becomes highly difficult. The flow characteristic around a circular cylinder is strongly influenced by the Reynolds number leading to well-known Karman vortex shedding. With rapid advancement in numerical methods and availability of better computing facilities, computations have been made on a single circular cylinder in the past several decades at a wide range of Reynolds number. A review of the studies made on the cylinder is dealt[1], where the flow is characterised by different regimes

based on Reynolds number. More details of the existing flow phenomena around a single circular cylinder obtained using experiments[2,8] and computations[3-5] have been reported in the literature. Effect of Reynolds number[5,7], turbulence model[4,6] is reported and indicates the complexity involved in the flow. Generally in the Hasan[9], *et al.* have demonstrated that by suitably modifying the boundary conditions, the domain could be reduced to 6 to 8 diameters without losing most of the flow features. Incorporation of such modified quantities at the boundary predicted the flow field reasonably well and made the computation more efficient due to the involvement of a lesser number of grids.

The placing of another cylinder either in tandem or side by side makes the flow more complex[10]. Such a situation is also encountered in many practical cases e.g. bundles of tubes of heat exchangers, high rise chimneys, and buildings, bridges, offshore structures, cooling towers of nuclear establishments, transmission cables, etc. Interference of flow field between cylinders becomes more severe when they are placed in tandem. The flow phenomena for these cases are governed by the gap between the two cylinders. The major factors influencing the overall flow field are the diameter of the cylinder, the gap between the two cylinders[11,12], Reynolds number[11,13,14], the number of cylinders[11], stagger angle[12], etc.

In the present investigation, an attempt has been made to study the incompressible flow around two circular cylinders of different diameters placed in tandem at a fixed distance using two - dimensional simulations. These simulations are the basic estimation of the existing flow field around two cylinders at different gaps and the results obtained can be used effectively by the researchers. The concept of the smaller domain (reported by Hasan[9]) has been used for the cases of a single cylinder, two cylinders of the same diameter and different diameters placed in proximity. To the best of our knowledge, such computational investigations using smaller domains for the case of cylinders are limited. The diameter of the upstream cylinder was varied such that it was either smaller or same or larger than the downstream cylinder.

2. NUMERICAL SCHEME

For two-dimensional incompressible viscous flows, the continuity and two momentum equations are:

$$\frac{\partial u}{\partial x}+\frac{\partial v}{\partial y} = 0 \tag{1}$$

$$\frac{\partial u}{\partial t}+\frac{\partial (u^2)}{\partial x}+\frac{\partial (uv)}{\partial y}=-\frac{\partial p}{\partial x}+\frac{1}{\mathrm{Re}}\times\left(\frac{\partial^2 u}{\partial x^2}+\frac{\partial^2 u}{\partial y^2}\right) \tag{2}$$

$$\frac{\partial v}{\partial t}+\frac{\partial (uv)}{\partial x}+\frac{\partial (v^2)}{\partial y}=-\frac{\partial p}{\partial y}+\frac{1}{\mathrm{Re}}\times\left(\frac{\partial^2 v}{\partial x^2}+\frac{\partial^2 v}{\partial y^2}\right) \tag{3}$$

These equations have been discretised using explicit finite volume technique. The physical region is divided into elementary quadrilateral cells. The integration is performed inside these quadrilateral cells. Laplace equation was used to generate the structured O-grid.

For the calculation of cell face velocities, a 'Consistent Flux Reconstruction' technique has been formulated. This is based on solving the momentum equations at each cell face. The present solver is based on the concept of the consistent physical interpolation (CPI) scheme.

The closures for the cell face center velocities u_e, v_e, u_n, v_n, u_w, v_w, u_S and v_S are derived by writing the discretised u and v components of the momentum equations at the points e, n, w and s, respectively. The discretisation of the unsteady term, convective term, pressure term and diffusive term at the point 'e' are given by Eqns. (4) to (7):

$$\iint_{\Omega_e}\left(\frac{\partial u}{\partial t}\right)_e d\Omega_e=\left(\frac{\partial u}{\partial t}\right)_e\times a_e=\left(\frac{u_e^{n+1}-u_e^{n}}{\Delta t}\right)\times 0.5\times\left(a_{_P}+a_{_E}\right) \tag{4}$$

$$\begin{aligned}\iint_{\Omega_e}\left[\frac{\partial}{\partial x}\left(\frac{\partial u}{\partial x}\right)+\frac{\partial}{\partial y}\left(\frac{\partial u}{\partial y}\right)\right]_e d\Omega_e &= \oint_{C_e}\left[\left(\frac{\partial u}{\partial x}\right)\times dy-\left(\frac{\partial u}{\partial y}\right)\times dx\right]\\ =\left(\frac{\partial u}{\partial x}\right)_E\times\Delta y_{es,en}+\left(\frac{\partial u}{\partial x}\right)_3\times\Delta y_{en,n}+\left(\frac{\partial u}{\partial x}\right)_P\times\Delta y_{n,s}+\left(\frac{\partial u}{\partial x}\right)_4\times\Delta y_{s,es}&\\ -\left(\frac{\partial u}{\partial y}\right)_E\times\Delta x_{es,en}-\left(\frac{\partial u}{\partial y}\right)_3\times\Delta x_{en,n}-\left(\frac{\partial u}{\partial y}\right)_P\times\Delta x_{n,s}-\left(\frac{\partial u}{\partial y}\right)_4\times\Delta x_{s,es}&\\ +O(|r_{12}|^3,.....)=UDFLUXe\end{aligned} \tag{5}$$

$$\begin{aligned}\iint_{\Omega_e}\left(\frac{\partial (uu)}{\partial x}+\frac{\partial (vu)}{\partial y}\right)_e d\Omega_e &= \oint_{C_e}\left((uu)\times dy-(vu)\times dx\right)\\ =u_E^2\times\Delta y_{es,en}-v_E\times u_E\times\Delta x_{es,en}+u_3^2\times\Delta y_{en,n}-v_3\times u_3\times\Delta x_{en,n}&\\ +u_P^2\times\Delta y_{n,s}-v_P\times u_P\times\Delta x_{n,s}+u_4^2\times\Delta y_{s,es}-v_4\times u_4\times\Delta x_{s,es}&\\ +O(|r_{12}|^3,.....)=UCFLUXe\end{aligned} \tag{6}$$

$$\begin{aligned}\iint_{\Omega_e}\left(\frac{\partial p}{\partial x}\right)_e d\Omega_e &= \oint_{C_e} p\times dy=p_E\times\Delta y_{es,en}+p_3\times\Delta y_{en,n}\\ +p_P\times\Delta y_{n,s}+p_4\times\Delta y_{s,es}+O(|r_{12}|^3,.....)&=UPFLUXe\end{aligned} \tag{7}$$

where $O(|r_{12}|^3,....)$ is the Newton-Cotes integration error.

$$\phi_1=\frac{(a_W+a_P)^2\times(a_{SW}\,\phi_S+a_S\,\phi_{SW})+(a_{SW}+a_S)^2\times(a_W\,\phi_P+a_P\,\phi_W)}{(a_{SW}+a_S)\times(a_W+a_P)\times(a_W+a_P+a_S+a_{SW})} \tag{8}$$

The first order velocity derivatives $(\partial\phi/\partial x)$ and $(\partial\phi/\partial y)$ at integration point E are obtained using Taylor series expansion which is given in Eqns. (9) and (10).

$$\left(\frac{\partial\,\phi}{\partial\,x}\right)_E=\frac{(\phi_{ee}-\phi_e)\times\Delta y_{es,en}-(\phi_{en}-\phi_{es})\times\Delta y_{e,ee}}{\Delta x_{e,ee}\times\Delta y_{es,en}-\Delta x_{es,en}\times\Delta y_{e,ee}} \tag{9}$$

$$\left(\frac{\partial \phi}{\partial y}\right)_E = -\frac{(\phi_{ee}-\phi_e)\times\Delta x_{es,en}-(\phi_{en}-\phi_{es})\times\Delta x_{e,ee}}{\Delta x_{e,ee}\times\Delta y_{es,en}-\Delta x_{es,en}\times\Delta y_{e,ee}} \quad (10)$$

The velocity derivatives at the other integration points and on other cell face centres (*n, w,* and *s*) are calculated using similar formulae. The closure interpolation formula for u_e is derived by substitution of Eqns. (4) to (7) into the integral form of Equation. The resulting expression for u_e at the $(n+1)^{th}$ time level is obtained as:

$$u_e^{n+1} = u_e^n + \frac{1}{0.5\times(a_P+a_E)}\times\begin{pmatrix}-UCFLUXe-UPFLUXe\\+UDFLUXe\end{pmatrix}\times\Delta t \quad (11)$$

The equation for pressure is derived by substituting the expressions for the reconstructed cell face center velocity components in the discretised continuity equation. On the solid surface, the pressure is obtained by applying zero normal gradients. The free stream pressure boundary condition is applied at the outer boundary. The pressure Poisson equation is solved using successive over relaxation scheme.

The governing equations are parabolic with respect to time and elliptic with respect to space. The pressure field and uniform free stream velocity are prescribed in each cell of the flow domain as an initial condition. At the inlet, free stream velocity has been imposed. At the outlet boundary, both transverse and the streamwise components are obtained by applying the continuity boundary condition. On the body surface, no-slip zero velocity boundary condition is applied. Similar methods have been adopted[18]. Flow past a single cylinder with a circular domain of 26 times the diameter of the cylinder using the Consistent Flux Reconstruction Scheme. Hasan[9], *et al*. has demonstrated that adoption of modified boundary condition at the outflow boundary leads to a reduction of the domain to the extent of the order of 6 to 8 diameter of the cylinder. It is reported that the results are comparable with the results obtained with conventional Neumann boundary condition having a larger domain. The major advantage of adopting modified boundary condition is the use of less number of grids and hence faster computation. For a polar structured grid, the extrapolated boundary conditions are given by Eqn. (12).

$$\left.\begin{aligned}(V_r)_2 &= \left[\frac{r_1}{r_2}\right]^2(V_r)_1+(V_r)_\infty\left\{1-\left[\frac{r_1}{r_2}\right]^2\right\}\\(V_\theta)_2 &= \left[\frac{r_1}{r_2}\right]^2(V_\theta)_1+(V_{\theta\infty})_2\left\{1-\left[\frac{r_1}{r_2}\right]^2\right\};\text{if }\Gamma=0\\\Gamma &= \begin{bmatrix}2\\\mu\end{bmatrix}\begin{bmatrix}\partial\mu\\\partial\eta\end{bmatrix}\end{aligned}\right\} \quad (12)$$

where v_r, v_θ, Γ, p are the radial velocity, circumferential velocity, circumferential component of circulation and pressure respectively. r_2 is the radius of the outer boundary domain and r_1 is the radius adjacent to the boundary. More details are available[9]. This boundary has been also implemented in the algorithm and has been used for making present computation around single or two cylinders.

The convergence criteria of the pressure Poisson equation is fixed as 10^{-5}. A strict convergence criterion for the pressure equation ensures a rapid reduction of the mass residual in the Continuity Equation. The history of the normalised RMS mass residual was observed during the computation to ensure that solution has converged. A typical 'O' domain has been used for the present computation where the left half is inflow and right half is outflow. The detail of the domain used for the computation has been specified during the discussion of results.

For all the computation, uniform free stream velocity and pressure field are prescribed at each cell as starting condition. No slip condition on the solid surface was enforced. Computation is made by specifying Dirichlet condition at outer boundaries when the boundary was large (order of 20 times the diameter of cylinder). In the case of using a smaller domain, convective boundary condition was enforced.

3. RESULTS AND DISCUSSION

3.1 Simulations over a Single Cylinder

Computation on a single cylinder was performed using the conventional boundary condition at a Reynolds number of 100 and a domain size of 26 D. A grid size of 160 x 120 was used for the present computation that was arrived at after a suitable grid independence test. The obtained result had a reasonable comparison with the results reported in the literature[3,15,16]. Further computations were made using the present solver with a larger domain size of 20 D having a similar grid distribution of 160 x 120. Figure 1(a) shows the instantaneous vorticity and streamline contours at non - dimensional time of t = 250 s, which depicts the overall flow features. Using the time history

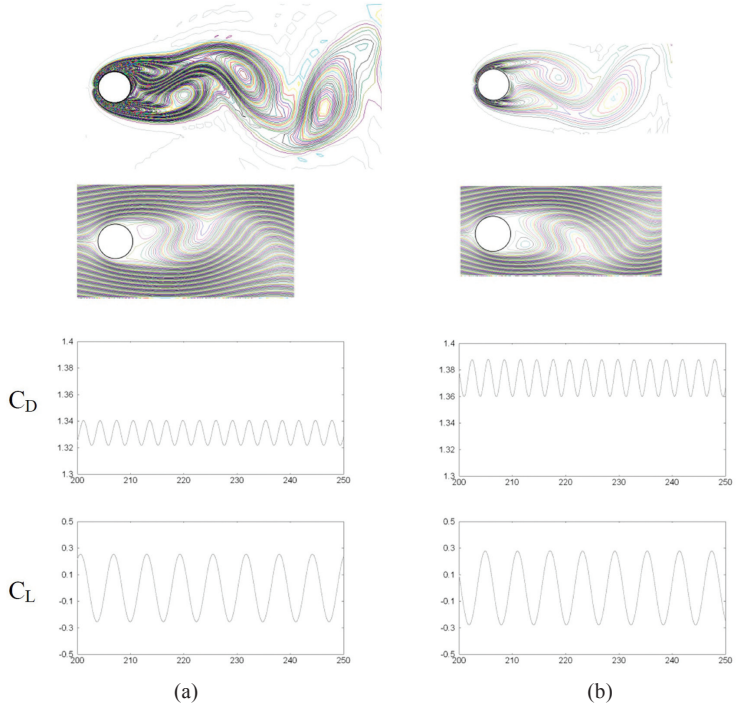

Figure 1. Vorticity, Streamline and time history of C_L and C_D for single cylinder at Re = 100 and using domain of (a) 20D and (b) 6D.

of C_L and C_D, presented in Fig. 1(a), the value of averaged C_L, C_D and Strouhal number are obtained, which are the main quantities used for validation. Table 1 shows a reasonable agreement of the present computation (larger domain of 20D) with the reported values in literature.

Table 1. Comparison of results for single cylinder at Re = 100

Study	C_D	Strouhal No.
Braza[3]	1.30	0.16
Menghini[15]	1.37	0.165
Harimi[16]	1.344	0.165
Proposed (domain of 20D)	1.33	0.16
Hasan[9] (using smaller domain of 6D)	1.424	0.166
Proposed (domain of 6D)	1.37	0.165

Once, the comparison of the results on a single cylinder indicated a good comparison, further computation with a smaller domain (6D) was made adopting convective boundary condition as suggested by Hasan[9]. The grid adopted was 121 x 60 which was arrived by reducing the number of grids in the radial direction relative to the reduction in the domain size. The results obtained for this case is shown in Fig. 1(b) and the derived quantities are shown in Table 1. The comparison indicates that the values obtained with the smaller domain are comparable to the results obtained for the larger domain and has the advantage of using around 37 per cent lesser grids and hence lesser computation time is required for the solutions. In addition, at the same instances, the flow obtained for both the cases of smaller and a larger domain seemed to be in reasonable agreement (Fig. 1). Variation of drag and lift with time were found to be in better agreement with the results obtained with the larger domain (Fig. 1), and the results are in line with the conclusion of Hasan[9]. The comparison of computed pressure distribution shown in Fig. 2 indicates that the use of smaller domain with convective boundary condition does not lead to appreciable differences in the overall flow field prediction for a single cylinder. A good agreement of pressures around the cylinder obtained using the present computations and measured values Homann, 1936 (reported[5] for Re = 107) was observed.

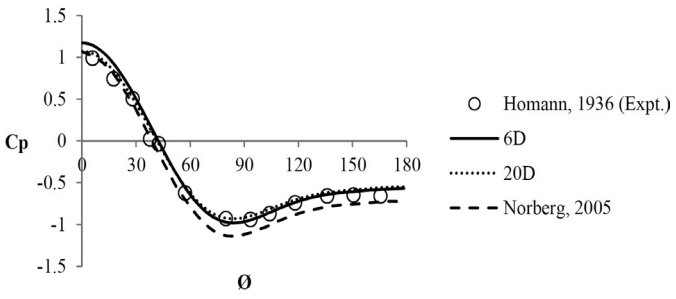

Figure 2. Pressure distribution around the cylinder for domain of 6D and 20D

3.2 Simulations over Two Cylinders of the same Diameter in Tandem

To ensure the suitability of the present solver for the case of two cylinders, an attempt has been made to validate the available result for two cylinders having the same diameter placed in tandem at a distance of 2L and at a Reynolds number of 200 (results reported[15,16]). The computation was made for the same conditions with larger domains of 40D and 20D using the grid of 300 x 145 and 300 x 120 respectively.

The computed instantaneous vorticity contour, streamline and time history of C_{L1}, C_{L2}, C_{D1} and C_{D2} is presented in Fig. 3(a) and Fig. 3(b). The comparison of averaged C_{L1}, C_{L2}, C_{D1} and C_{D2} and the Strouhal number presented in Table 2 indicates reasonable comparison with the results reported[15,16]. For larger domain size, the averaged C_{D1} is in agreement within 5 per cent, whereas C_{D2} differs by about 10 per cent - 15 per cent, which may be due to the difference in grids and their distribution and as well its value being very small. Differences were observed in the strouhal number which likely due to the differences in the grids or the boundary conditions. This can only be confirmed using excellent experimental data.

Table 2. Comparison of results for two cylinders of same diameter at Re = 200

Study	C_{D1}	C_{D2}	C_{L1}	C_{L2}	Str_1	Str_2
Meneghini[15]	1.03	-0.17	-0.001	0.00	0.130	0.130
Harimi[16]	1.03	-0.17	-	-	-	-
Ghadiri[19], *et al*.	1.03	-0.16	-	-	0.138	0.138
Slaouti and Stansby[17]	0.89	-0.21	-	-	0.130	0.130
Proposed (40D)	1.00	-0.19	0.00	0.00	0.16	0.16
Proposed (20D)	0.985	-0.185	-0.001	-0.001	0.16	0.16
Proposed (15D)	0.97	-0.181	-0.002	-0.002	0.16	0.16
Proposed (8D)	0.887	-0.165	-0.006	-0.008	0.145	0.145

Once the results obtained with larger domain was found to be in reasonably good agreement, an attempt was made to make computation adopting modified boundary conditions for the smaller domain as done in the case of a single cylinder. For the single cylinder, it has been found that use of a domain of 6D captured most of the flow field features and hence the same was enforced for computation for two cylinders. This has lead to the use of domain of 8D, which is still quite less than the usual boundary domain of 20D. For the sake of completion, computation has also been made with a domain of 15D. The grids used for 15D and 8D were 300x110 and 300x90 respectively. The computed results obtained with these grids adopting modified boundary condition is presented in Fig. 3(c) and Fig. 3(d). Comparison of results indicates that most of the features are captured even with the use of domain of 8D. Formation of the separation bubble in the rear of the upstream cylinder, the formation of the wake in the rear of the downstream cylinder was similar to the results reported in the literature. Hence, the current solver with the modified boundary condition was expected to yield good results. The averaged value of C_{L1}, C_{L2}, C_{D1} and C_{D2} and the Strouhal number is presented in Table 2. In general, the results are reasonable

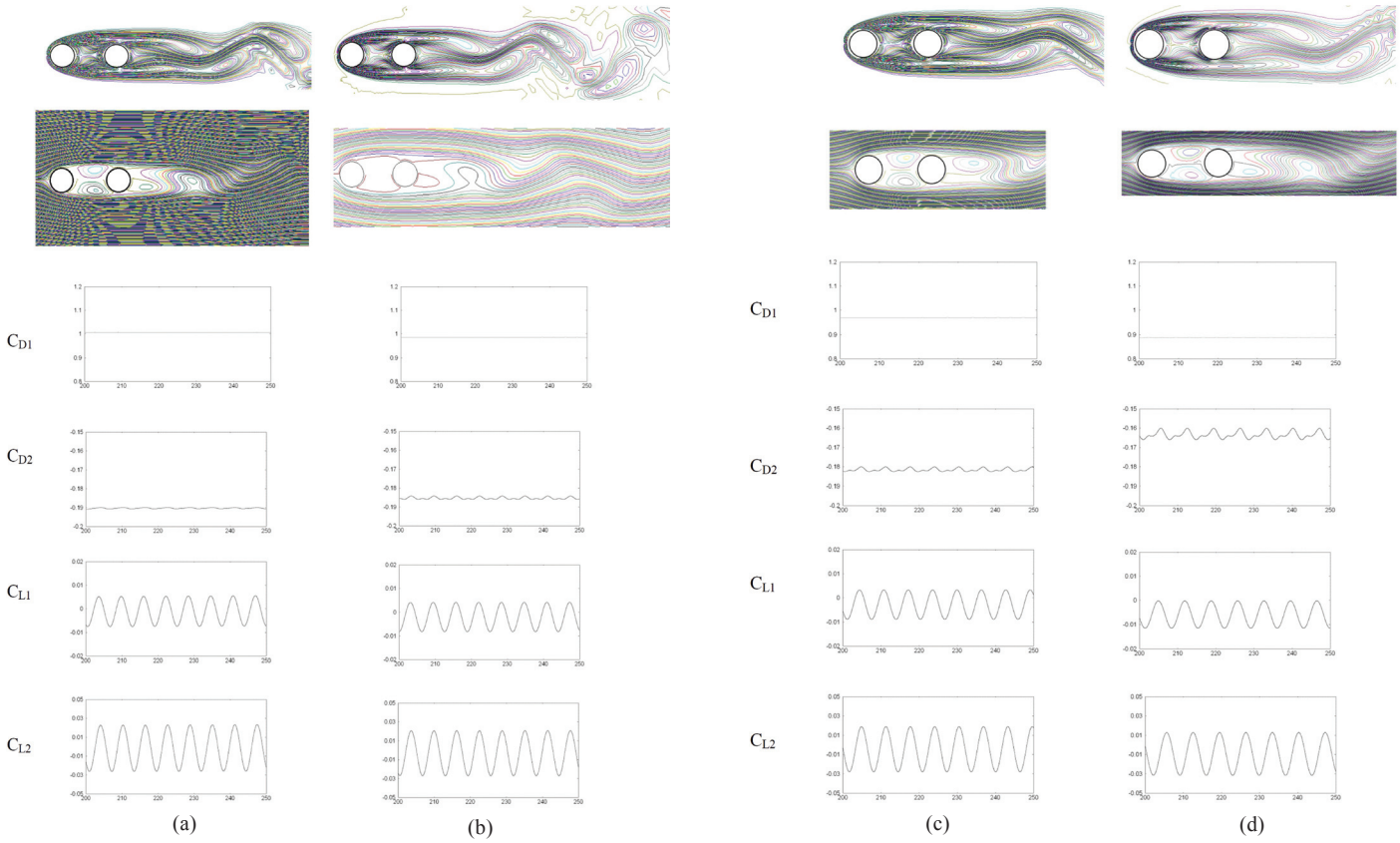

Figure 3. Vorticity, Streamline, time history of C_L and C_D for two cylinders of same diameter(D-D) at Re = 200 and G=2L: (a) 40D (b) 20D, (c) 15D, and (d) 8D.

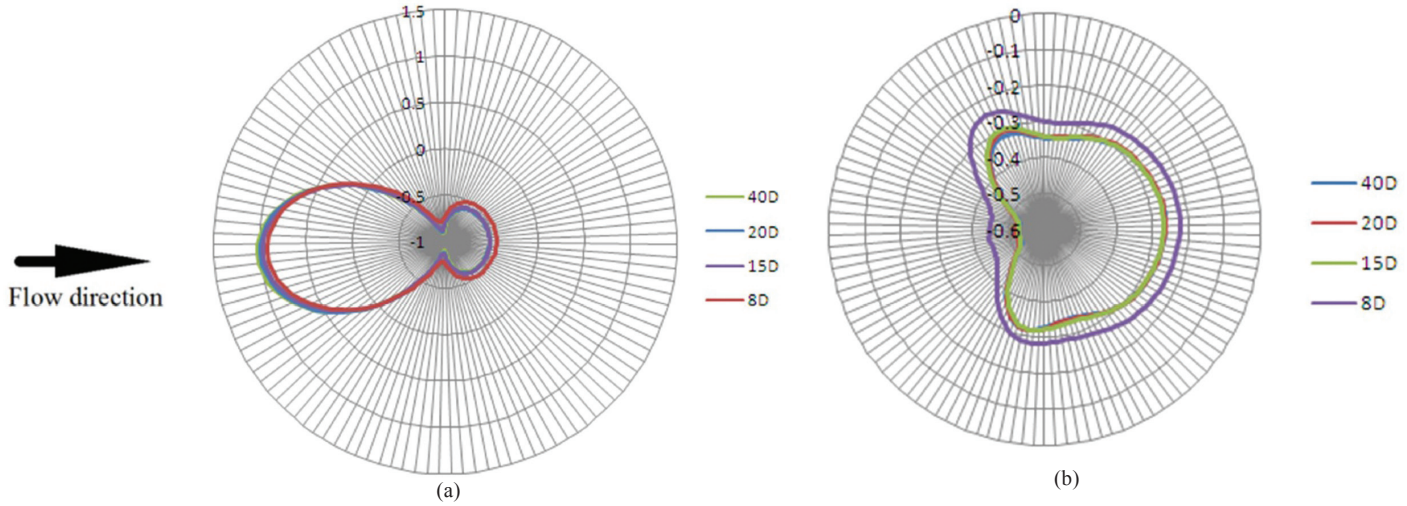

Figure 4. Pressure distribution on two cylinders of same diameter (D-D) at Re = 200 and G=2L: (a) Upstream cylinder and (b) Downstream cylinder.

except for C_{D2}, where it predicts a lower value. The comparison of pressure distribution for different domains is as shown in Fig. 4, which indicates a similar trend. The effect of reducing the domain is more predominant on the downstream cylinder in comparison of the upstream cylinder. However, the trend is still similar. Possibly, the modification in the grid distribution could lead to a better agreement. The results indicate that the use of modified boundary condition established for single cylinder could also be successfully implemented for computation around two cylinders with 20 per cent lesser grids.

In the present investigation, it has been planned to obtain the flow around a pair of cylinders placed in tandem at a gap G= 3L at Re = 100. Therefore, initially, the computation has been made for cylinders of the same diameter at this Reynolds number. The results obtained with a domain size of 20D, 15D, and 9D is presented in Fig. 5 and the grid adopted was 300 x 120, 300 x 110 and 300 x 90 respectively. For the domain of 15D and 9D, the modified boundary condition was enforced. Comparison of Figs. 3(b)-3(d) with 5(a)-5(c) indicates the change in an overall flow field with a change in Reynolds

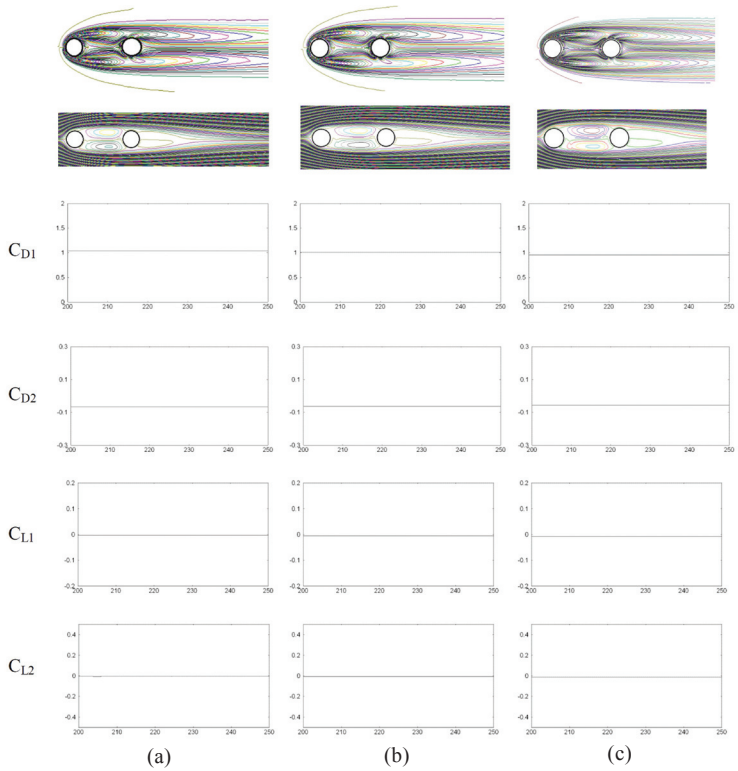

Figure 5. Vorticity, Streamline, time history of C_L and C_D for two cylinders of same diameter (D-D) at Re = 100, G=3L: (a) 20D, (b) 15D, and (c) 9D.

number and the gap between the two cylinders. Interestingly, no oscillations are observed in C_{L1} and C_{L2} at the gap of 3L indicating the absence of unsteady vortex formation in the flow. This could be seen from streamline contour as well. Here also, it is observed that reduction of the domain of boundary with the adoption of modified boundary condition does not lead to any major loss of flow field. The flow features are almost similar to the flow observed with a larger domain of 20D. Comparison of values presented in Table 3 indicates that the values obtained with a smaller domain with modified boundary are in reasonable agreement for the upstream cylinder in comparison to the downstream cylinder. The comparison with results[16] also indicates reasonably good comparison. The pressure distribution presented in Fig. 6 also shows a similar distribution with different domains of 20 D, 15 D, and 9 D.

3.3 Simulations over Two Cylinders of Different Diameters in Tandem

The computation around cylinders of the same diameter indicated that smaller domain gives a reasonably good result. Hence, further computation was made to obtain the flow field around cylinders of different diameters placed in tandem at a gap G = 3L and Re = 100 based on the diameter of a cylinder placed in the downstream direction. For the present computation, the diameter of the upstream cylinder (D_1) was varied such that either it was less or equal or larger than the diameter of a cylinder placed downstream (D_2). Therefore, the diameter of the downstream cylinder (D_2) has been designated as D and the diameter of the upstream cylinder (D_1) was varied as 0.5 D, 0.667 D, 1D, 1.5D and 2 D, which covers the range of either placing a smaller or larger diameter cylinder upstream of a cylinder. The gap between the cylinders was maintained as (G=3L) i.e. three times the average diameter of the cylinders. All the computation has been made adopting smaller domain with the modified boundary condition. Therefore, the domain size varied for each case. It was ensured that for the selected domain, the distance between any cylinder and domain boundary is not less than six times the diameter of that particular cylinder (based on the results obtained from the single cylinder). The details of minimum values of X_1 and X_2

Table 3. Lift and drag coefficient for two cylinders of the same diameter at 3L and Re = 100

Domain	C_{D1}	C_{D2}	C_{L1}	C_{L2}	Str_1	Str_2
Harimi[16]	1.16	0.003			--	-
20D	1.035	-0.066	-0.003	-0.004	--	-
15D	1.01	-0.062	-0.004	-0.006	-	-
9D	0.952	-0.057	-0.006	-0.009	-	-

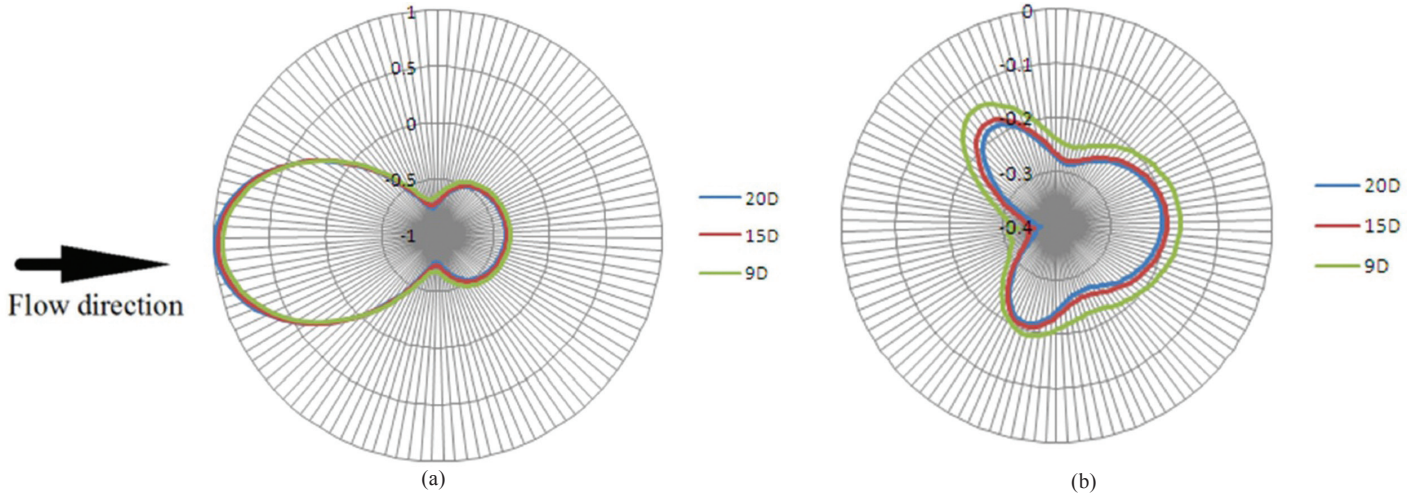

Figure 6. Pressure distribution on cylinders with different domains for two cylinders of same diameter (D-D) at Re = 100, G=3L (a) Upstream cylinder and (b) Downstream cylinder.

for different combinations and hence the domain to be adopted for computation is as shown in Table 4.

Although the results for case 3 [i.e. cylinders of the same diameter (D-D)] has already been presented and discussed, some of the results are again included here. Figures 7(a-e) shows the details of flow field obtained for all the cases which clearly shows the effect of diameter of the upstream cylinder. The streamline observed for case-1 (2D-D) presented in Fig. 7(a) indicates similarity with the flow over a single cylinder, indicating that downstream cylinder is engulfed in the wake of the upstream cylinder. Based on the diameter, the upstream cylinder faces a Reynolds number of 200 due to which the complexity of the flow increases and a drag coefficient of 1.71 is observed. While the downstream cylinder experiences a negative drag as it is surrounded inside the wake of the upstream cylinder. With the reduction in diameter of the upstream cylinder to 1.5D (case-2), change in streamline and vorticity contour is observed. From Fig. 7(b), it is observed that the wake of the upstream cylinder reduces due to which the drag of the upstream reduces while the drag of the downstream cylinder starts increasing. For the case of the same diameter, no oscillations were observed as discussed previously. With a further decrease in upstream diameter, the Reynolds number of the upstream cylinder decreases. The wake of the first cylinder further reduces leading to further decrease in the drag of the upstream cylinder. Due to this, the interference of the wake on the oncoming flow of the downstream cylinder decreases. This leads to the increase in the drag of the downstream cylinder. Since the unsteady vortex shedding again establishes, the oscillation in the lift and drag again starts. Further, decrease in the diameter of the upstream cylinder to 0.5D decreases the drag on the upstream cylinder and further increases the drag on the downstream cylinder. Moreover, the upstream cylinder faces a Reynolds number of 50 at which the shedding

Table 4. Details of configurations and domain adopted for computation

Case No.	Diameter of cylinders		Gap G = 3L [L=(D_1+D_2)/2]	Minimum (X_1)	Minimum (X_2)	Computation Domain
	Upstream (D_1)	Downstream (D_2=D)				
1	2D	D	4.5D	12D	6D	12D
2	1.5D	D	3.75D	9D	6D	10D
3	D	D	3D	6D	6D	9D
4	0.667D	D	2.5D	4D	6D	9D
5	0.5D	D	2.25D	3D	6D	9D

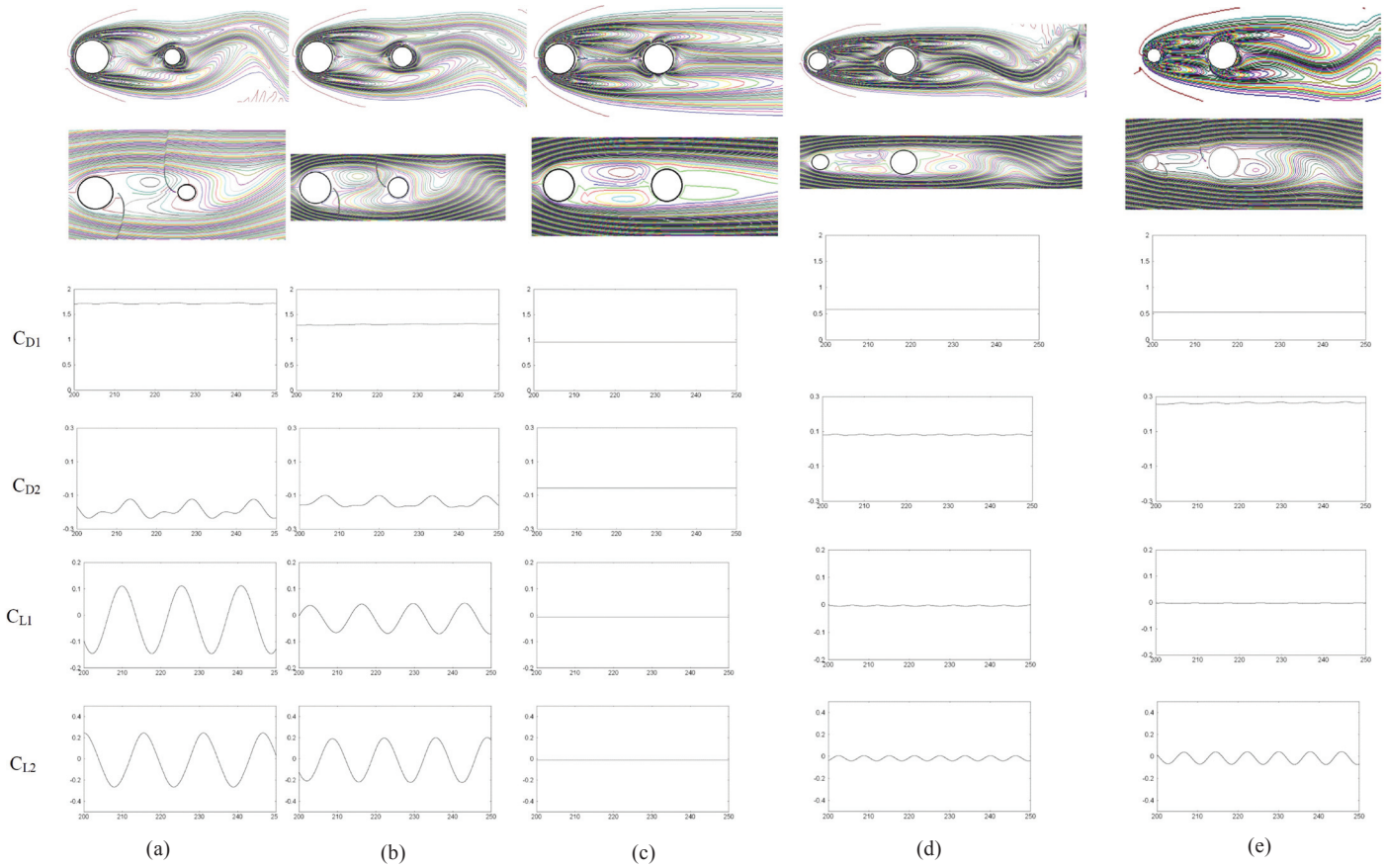

Figure 7. Vorticity, Streamline, time history of C_L and C_D for two cylinders of different diameters (D_1-D_2) at Re = 100, G=3L: (a) 2D-D, (b) 1.5D-D, (c) D-D, (d) 0.67D-D, and (e) 0.5D-D

process is just expected to start. Due to this, a decrease in the strouhal number is also observed. The effect of diameter of the upstream cylinder could be better visualised from the vorticity contours presented in Fig. 8. The pressure distribution on both the cylinders is presented in Fig. 9, which indicates that the effect on the downstream cylinder is more predominant with a change in diameter of the upstream cylinder. The averaged value of C_{D1}, $C_{D2}$and C_{L1}, C_{L2} obtained from these results is presented in Table 5 which indicates that the value of C_{D1} reduces with a decrease in D_1. However, the change is small, when the diameter of the upstream cylinder is smaller than the diameter of the downstream cylinder. Except for 2D-D case, the value of C_{D1} is always less than the value of a single cylinder. This could be due to change in the flow pattern in the interference zone. The observed value of C_{D2} indicates an increase in drag with a decrease in the diameter of the upstream

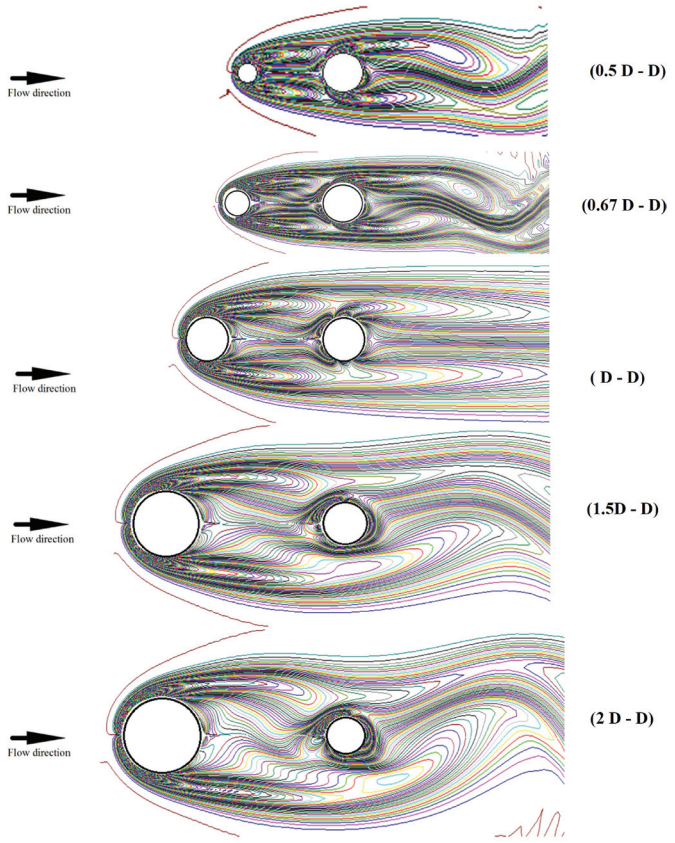

Figure 8. Vorticity contour for two cylinders of different diameters (D_1-D_2) at Re = 100, G=3L.

Table 5. Lift and drag coefficients for cylinders of different diameters at a distance of 3L

Cases		C_{D1}	C_{D2}	C_{L1}	C_{L2}	Str_1	Str_2
1	2D-D	1.71	-0.189	-0.01	0.012	0.06	0.067
2	1.5D-D	1.31	-0.148	-0.01	-0.011	0.07	0.07
3	D-D	0.952	-0.057	-0.006	-0.009	-	-
4	0.667D-D	0.577	0.08	-0.003	-0.017	0.16	0.16
5	0.5D-D	0.53	0.26	-0.002	-0.015	0.125	0.125
6	D	1.37	--	0.00	---	0.165	

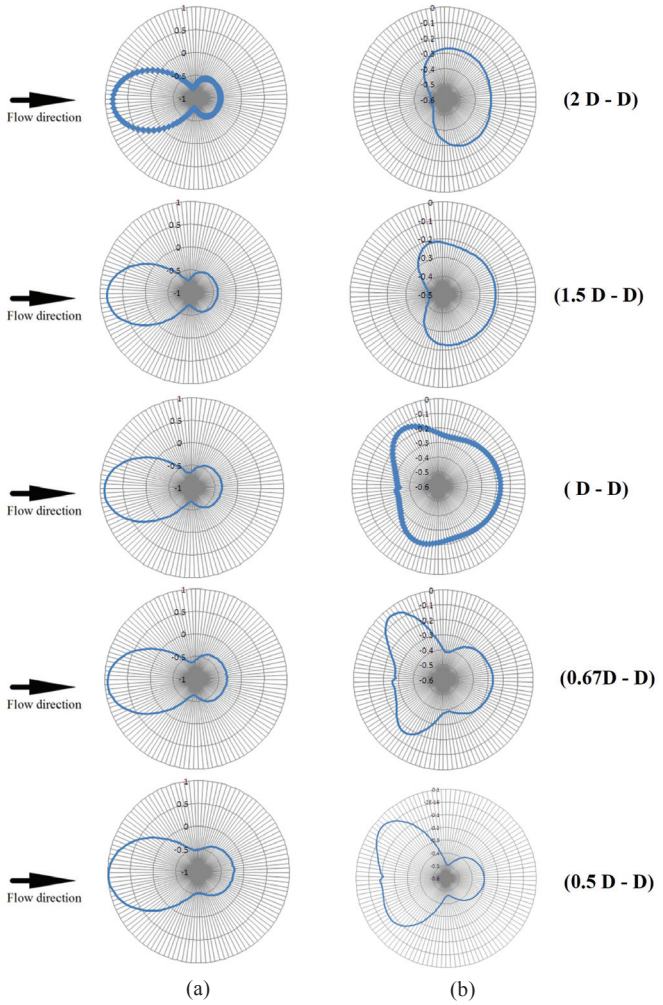

Figure 9. Pressure distribution on cylinders of different diameters (D_1-D_2) at Re = 100, G=3L (a) Upstream cylinder and (b) Downstream cylinder.

cylinder. It is also to be noticed that average value of C_D for a single cylinder is around 1.34. The value of C_{D2} is observed to be 0.26 in the presence of a small cylinder (case-5), indicating the reduction of drag could be achieved by mounting a small cylinder in the upstream direction. With the increase in the diameter of the upstream cylinder, the drag of downstream cylinder decreases and attains negative value. This could be due to the strong influence of larger wake of the upstream cylinder on the downstream cylinder. The Strouhal number does not seem to be predominantly affected by the change in diameter of the cylinder and found to be always less than the value observed for a single cylinder. These results are better visualised from the results presented in Fig. 10. These results suggest that use of smaller domain does not lead to major loss of flow features. Hence, this could be used to obtain overall behavior of flow field followed with final computation with a larger number of grids and domain.

4. CONCLUSIONS

A two-dimensional Navier-Stokes solver based on finite volume approach using a boundary-fitted curvilinear structured O-grid has been developed to obtain details of unconfined flow past cylinders at low Reynolds number of 100 and 200. The

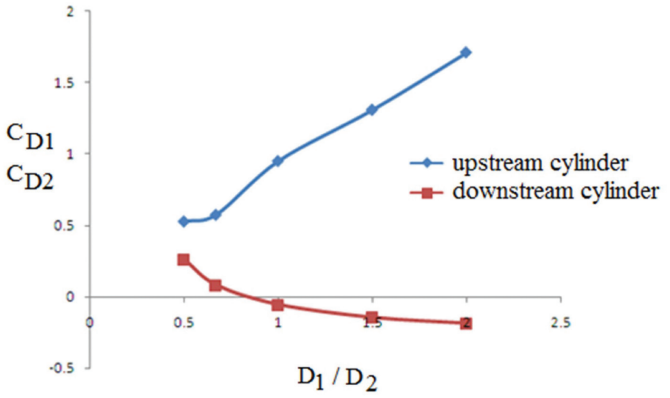

Figure 10. Effect of diameter ratio (D_1/D_2) on drag coefficient at Re = 100, G=3L.

algorithm developed has the capability to enforce convective boundary conditions. Computation has been made on a single cylinder at Reynolds number of 100 adopting conventional large domain of 20 times the diameter and as well with a domain of 6 times the diameter with the implementation of convective boundary condition. It is observed that adoption of the small domain with convective boundary condition captures most of the flow features and has the advantage of using almost 37 per cent lesser number of grids and hence reduces the computational time. Similar computations made over two cylinders of the same diameter placed in tandem also indicated that smaller domain with suitable boundary conditions could be successfully used to obtain the flow field and found to give satisfactory results with a grid reduction of about 20 per cent – 25 per cent. Computation over two cylinders of different diameters placed at a distance in tandem has been made adopting modified boundary condition. It is observed that with a change in diameter of the upstream cylinder, the overall flow field changes. The flow field in the interference region and as well on the downstream cylinder is strongly influenced. The drag of the downstream cylinder decreases with increase in diameter of the upstream cylinder. It is demonstrated that the adoption of modified boundary condition leads to a reduction in the number of grids and computation time. Hence, it could be used initially before making the final computation with larger domain and finer grids for final computation.

REFERENCES

1. Zdravkovich, M.M. Flow around circular cylinders. Oxford Science Publications, Oxford University Press, Oxford, UK, 1997, **1**, 672.
2. Roshko, A. On the drag and shedding frequency of two-dimensional bluff bodies. National Advisory Committee for Aeronautics, Report No. NACA-TN-3169. July 1954.
3. Braza, M.; Chassaing, P. & Minh, H.Ha. Numerical study and physical analysis of the pressure and velocity fields in the near wake of a circular cylinder. *J. Fluid Mech.*, 1986, **165**, 79-130. doi:10.1017/S0022112086003014
4. Lu, X.; Dalton, C. & Zhang, J. Application of large eddy simulation to an oscillating flow past a circular cylinder. *J. Fluid Eng.*, 1997, **119**(3), 519-527, doi:10.1115/1.2819275
5. Rajani, B.N.; Kandasamy, A. & Mazumdar, S. Numerical simulation of laminar flow past a circular cylinder. *Appl. Math. Model.*, 2009, **33**(3), 1228-1247. doi: 10.1016/j.apm.2008.01.017
6. Anal, U.O.; Altar, M. & Goren, O. Effect of turbulence modeling on the computation of the near wake flow of acircular cylinder. *Ocean Eng.*, 2010, **37**(4), 387-389. doi: 10.1016/j.oceaneng.2009.12.007
7. Norberg, C. Fluctuating lift on a circular cylinder: review and new measurements. *J. Fluid Struct.*, 2003, **17**(1), 57-96. doi: 10.1016/S0889-9746(02)00099-3
8. Homann, F. Influence of higher viscosity on flow around cylinder. National Advisory Committee for Aeronautics, Report No. NACA-TM-1334. June 1952.
9. Hasan, N.; Anwer, S.F. & Sanghi, S. On the outflow boundary condition for external incompressible flows: A new approach. *J. Comput. Phy.*, 2005, **206**(2), 661-683. doi: 10.1016/j.jcp.2004.12.025
10. Zdravkovich, M.M. Review of flow interference between two circular cylinders in various arrangements. *J. Fluid Eng. ASME*, 1977, **99**(4), 618-633. doi: 10.1115/1.3448871
11. Zdravkovich, M.M. The effects of interference between circular cylinders in cross flow. *J. Fluids Struct.*, 1987, **1**(2), 239-261. doi: 10.1016/S0889-9746(87)90355-0
12. Sumner, D. Two cylinders in cross flow; A review. *J. Fluids Struct.*, 2010, **26**(6), 849-899, doi: 10.1016/j.jfluidstructs.2010.07.001
13. Gu, Z.F. On interference between two circular cylinders at supercritical Reynolds number. *J. Wind Eng. Ind. Aerodyn.*, 1997, **62**(2), 175-190. doi: 10.1016/S0167-6105(96)00056-6
14. Gu, Z.F. & Sun, T. On interference between two circular cylinders in staggered arrangement at high subcritical Reynolds numbers. *J. Wind Eng. Ind. Aerodyn.*, 1999, **80**(3), 287-309. doi: 10.1016/S0167-6105(98)00205-0
15. Meneghini, J.R.; Saltara, F.; Siqueira, C.L.R. & Ferrari Jr., J.A. Numerical simulation of flow interference between two circular cylinders in tandem and side-by-side arrangements. *J. Fluids Struct.*, 2001, **15**(2), 327–350. doi: 10.1006/jfls.2000.0343
16. Harimi, I. & Saghafian, M. Numerical simulation of fluid flow and forced convection heat transfer from tandem circular cylinders using overset grid method. *J. Fluids Struct.*, 2012, **28**, 309-327. doi: 10.1016/j.jfluidstructs.2011.12.006
17. Slaouti, A. & Stansby, P.K. Flow around two circular cylinders by the random-vortex method. *J. Fluids Struct.*, 1992, **6**(6), 641-670. doi: 10.1016/0889-9746(92)90001-J
18. Roy, A. & Bandyopadhyay, G. A finite volume method for viscous incompressible flows using a consistent flux reconstruction scheme. *Int. J. Numer. Meth. Fluids*, 2006, **52**(3), 279-319. doi: 10.1002/fld.1180

19. Ghadiri B.; Moghaddam, H.S. & Jafari, H.H. Numerical simulation of flow over two circular cylinders in tandem arrangement. *J. Hydro.,* 2011, **23**(1), 114-126. doi: 10.1016/s1001-6058(10)60095-9

CONTRIBUTORS

Dr Y.G. Bhumkar obtained his PhD from IIT Kanpur. He did his ME from BIT Mesra. Presently he is working as Assistant Professor at IIT Bhubaneswar. His research area includes advanced fluid mechanics, high performance computing for thermo-fluids applications.
In the current work is a part of his Thesis work which is the preliminary development of the current CFD code

Dr P. Kumar obtained his PhD in Engineering from Birla Institute of Technology, Mesra Ranchi. He is presently working as Assistant Professor at Department of Space Engineering and Rocketry, BIT Mesra. His research area includes Low speed aerodynamics, high angles of attack, experimental aerodynamics.
The further extension of the CFD code towards cylinder of various diameters, its solution and post processing work has been carried out by him.

Dr A. Roy obtained his PhD in Engineering from IIT Kharagpur. He has worked at BIT Mesra as an Assistant Professor before joining IIT Kharagpur as a faculty member. His research area includes computational fluid dynamics, single and multiphase fluid dynamics.
The initial development of code was carried out under his supervision.

Dr S. Das obtained his PhD in Engineering from Birla Institute of Technology, Mesra and a post-doc from Technion, Israel Institute of Technology. He is presently working as Professor at Department of Space Engineering and Rocketry, BIT Mesra. His research area includes High speed flows, shock boundary layer interaction, unsteady aerodynamics.
His contribution is towards the work related to grid generation, domain and its sensitivity towards multiple bodies.

Dr J.K. Prasad obtained his PhD (Aerospace Engg.) from IIT, Madras. Currently he is working as Director at Birla Institute of Technology, Deoghar Center, Jharkhand. His area of research include: Aerodynamics, jets, jet interactions, etc.
He was instrumental in the initial development of code in the capacity of a mentor.